Numerical Investigation of Corium Spreading Phenomena using Smoothed Particle Hydrodynamics

Hee Sang Yoo[a], and Eung Soo Kim[a*]
[a]*Department of Nuclear Engineering, Seoul National University 1 Gwanak-ro, Gwanak-gu, Seoul, South Korea*
[*]*Corresponding author: kes7741@snu.ac.kr*

***Keywords : SPH, Corium Spreading, ALE, Implicit Viscosity Solver**

1. Introduction

Understanding the intricate dynamics of molten corium spreading is critical for ensuring effective post-accident heat removal and preserving the structural integrity of reactor containment systems during severe nuclear incidents [1-2]. Corium spreading involves complex interactions of hydrodynamics, heat transfer, phase change, and potential chemical reactions. At initial stages, experiments were conducted with simulant materials due to low costs and constraints, but, these materials are evidently different from real corium. However, conducting experiments with real corium is expensive and challenging due to the difficult conditions.

To address experimental constraints, numerical methods are being actively adopted as a substantial option. Analytical approaches, though simple in certain cases, often fail to capture if the complexities of scenarios increase and provide limited data. Similarly, lumped parameter methods, while successful in correlating with experimental results, lack comprehensive information, particularly when constrained to 1D or 2D approaches.

Advancements in computing power have facilitated the adoption of computational fluid dynamics (CFD) techniques for studying corium spreading including grid-based methods like Finite Volume and Finite Element [1]. Recently, mesh-free methods have gaining prominence for their suitability in modeling free surface flows. Mesh-free methods including Moving Particle Semi-implicit (MPS) or Smoothed Particle Hydrodynamics (SPH) emerge as promising approaches for simulating corium spreading phenomena [2].

In this study, we employ the SPH method to investigate the intricate dynamics governing corium spreading phenomena. Our investigation unveils the capacity of SPH to yield comprehensive insights into heat transfer mechanisms and phase change phenomena. The applicability and efficacy of SPH method on corium spreading phenomena have been demonstrated through the VULCANO VE-U7 experiment.

2. Numerical method

The SPH stands out as one of the most well-known Lagrangian meshless CFD method. In this section, we briefly outline the basic concept of SPH and describe the discretized governing equations.

2.1 SPH approximation

The SPH convolution of a function $f(\boldsymbol{r})$ at the position $\boldsymbol{r}$ is defined as the integral over a support domain Ω around a point r with a smooth weighting function $W(\boldsymbol{r}-\boldsymbol{r}', h)$:

$$f(\boldsymbol{r}) = \int_{\Omega} f(\boldsymbol{r}')W(\boldsymbol{r}-\boldsymbol{r}', h)d\boldsymbol{r}', \quad (1)$$

where h represents the smoothing length, defined as $h = 1.5\Delta x$, with Δx being the grid spacing. kh denotes the radius of the domain of interest Ω, where k is the scale factor defining the effective area of the kernel smoothing function. In this study, k is set to 1.66 .In the discretized system, the function $f(\boldsymbol{r}_i)$ at the position of particle of interest $\boldsymbol{r}_i$ is expressed by:

$$f(\boldsymbol{r}_i) = \sum\nolimits_j f(\boldsymbol{r}_j)W_{ij}(\boldsymbol{r}_i - \boldsymbol{r}_j, h_i)V_j, \quad (2)$$

where the subscript j represents the neighboring particles of particle of interest, V_j is the volume of particle j and can be substituted into m_j/ρ_j. The basic principle of SPH convolution is illustrated in Fig.1.

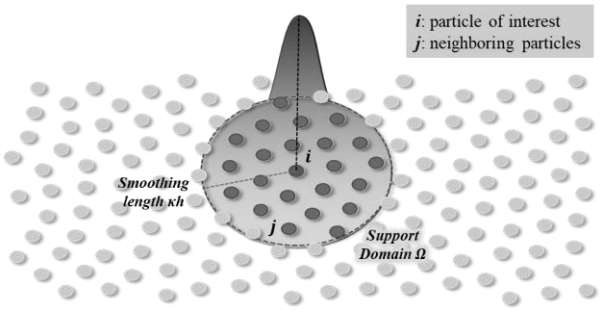

Fig. 1. Schematic view of SPH convolution

2.2 Discretized Governing Equations

The governing equations for incompressible flow encompass mass, momentum, and energy conservation equations. In this study, the Explicit Incompressible Smoothed Particle Hydrodynamics (EISPH) method is

employed to solve the discretized governing equations [3]. The discretized system for EISPH method for has been well described in prior studies. In EISPH method, the momentum equation is divided into two parts for solution.

Initially, forces excluding pressure force are computed to obtain intermediate velocity. Subsequently, the pressure field is determined based on the Pressure Poisson Equation (PPE). Following this, the pressure force is calculated to update the final velocity and position. Furthermore, as we consider heat, we need to solve the energy equation. The governing equations are listed in the Table 1.

Table I. EISPH governing equations

Momentum conservation	
$$\frac{\boldsymbol{Du_i}}{\boldsymbol{Dt}} = \boldsymbol{f}_{b,i} - \sum_j \boldsymbol{2\widetilde{P_{ij}}\nabla_i W_{ij}}\frac{\boldsymbol{m_j}}{\boldsymbol{\rho_i\rho_j}} + \sum_j \boldsymbol{2\overline{\nu_{ij}}u_{ji}}\frac{\boldsymbol{r_{ij}\cdot\nabla W(r_{ij},h)}}{\boldsymbol{r_{ij}^2}}\frac{\boldsymbol{m_j}}{\boldsymbol{\rho_j}}.$$	(3)
Pressure Poisson Equation (PPE)	
$$\boldsymbol{P_i^{n+1}} = \frac{\boldsymbol{b_i} + \sum_{j=1}^{N}\boldsymbol{A_{ij}(P_j^n)}}{\sum_{j=1}^{N}\boldsymbol{A_{ij}}}.$$	(4)
$$\boldsymbol{A_{ij}} := \boldsymbol{2}\frac{\boldsymbol{r_{ij}\cdot\nabla W(r_{ij},h)}}{\boldsymbol{r_{ij}^2}}\frac{\boldsymbol{m_j}}{\boldsymbol{\rho_j}} \quad \boldsymbol{b_i} := \frac{\overline{\boldsymbol{\rho_{ij}}}\sum_j \boldsymbol{u_{ji}^*\cdot\nabla W(r_{ij},h)}\frac{\boldsymbol{m_j}}{\boldsymbol{\rho_j}}}{\boldsymbol{\Delta t}}$$	(5)
Energy conservation	
$$\frac{\boldsymbol{DH_i}}{\boldsymbol{Dt}} = \sum_j \boldsymbol{2\overline{k_{ij}}H_{ji}}\frac{\boldsymbol{r_{ij}\cdot\nabla W(r_{ij},h)}}{\boldsymbol{r_{ij}^2}}\frac{\boldsymbol{m_j}}{\boldsymbol{\rho_i\rho_j}} - \frac{\boldsymbol{1}}{\boldsymbol{\rho_i}}[\boldsymbol{\sigma\varepsilon_i(T^4 - T_\infty^4)}]\boldsymbol{\delta_V}.$$	(6)

Where D t/D represents the Lagrangian derivative, $\boldsymbol{u}, P, T$, and H represent velocity, pressure, temperature, and enthalpy, respectively. $\boldsymbol{f}_b$ denotes the body force. ν, k , and ε signify kinematic viscosity, thermal conductivity, and emissivity, respectively. σ represents the Stefan-Boltzmann constant, δ_V denotes the interfacial function, and T_∞ represents the ambient temperature. The subscript ij signifies the interaction between particles i and j, while ji represents the reverse interaction. The upper bar and tilde indicates the inter-particle value between particle i and j.

2.3 Arbitrary Lagrangian-Eulerian (ALE) SPH

The conventional Lagrangian SPH method encounters challenges due to the irregular particle distribution inherent in its Lagrangian nature [4]. In this study, a consistent ALE-SPH scheme is adopted to mitigate the irregular particle distribution resulting from Lagrangian characteristics. Particles move with a transport velocity, which is defined as sum of the physical velocity u and a perturbation velocity term δu. When δu is zero, the motion is purely Lagrangian, and when it is equal to negative of the physical velocity u, the motion is entirely Eulerian. The displacement component δu is adjusted based on the distribution of particles but strictly constrained to be smaller than half of the magnitude of the velocity component. This results in a quasi-Lagrangian scheme in which the particle path deviates slightly from the traditional Lagrangian approach [4].

$$\nabla_i C_i = \sum_j \left[1 + 0.2\left(\frac{W_{ij}}{W_{ij}(\Delta x)}\right)^4\right]\frac{m_j}{\rho_j}\nabla_i W_{ij}. \tag{7}$$

$$\delta\boldsymbol{u}_i = \begin{cases} -\kappa h_i|\boldsymbol{u}_i|\nabla C_i & if\ |\kappa h_i|\boldsymbol{u}_i|\nabla C_i| < 0.5|\boldsymbol{u}_i|, \\ -0.5|\boldsymbol{u}_i|\dfrac{\nabla C_i}{|\nabla C_i|} & \text{otherwise,} \end{cases} \tag{8}$$

As the perturbation velocity $\delta\boldsymbol{u}$ is added, causing particles to move at a speed different from the physical velocity $\boldsymbol{u}$, the system is no longer purely Lagrangian. Therefore, the modified time derivative is rederived based on the new transport velocity ($\boldsymbol{u} + \delta\boldsymbol{u}$).

$$\frac{df}{dt} := \frac{\partial f}{\partial t} + (u + \delta\boldsymbol{u})\cdot\nabla f = \frac{Df}{Dt} + \delta\boldsymbol{u}\cdot\nabla f. \tag{9}$$

Here, ∂t/∂ represents the partial derivative. In this study, the governing equations are integrated in time based on modified time derivative. Given our utilization of an incompressible SPH method, we assume that density remains constant, and mass is also fixed.

2.4 Implicit Viscosity Solver

In explicit time integration, the time-step decreases anti-proportionally to viscosity to restrict viscous diffusion. Consequently, in severe accidents where corium experiences phase change from liquid to solid, viscosity increases drastically, leading to a significant decrease in time-step. As a result, the computational time becomes prohibitively expensive. Therefore, we implemented an implicit viscosity solver based on GPU parallelization to efficiently compute highly viscous corium in this study.

In the implicit time integration of the viscous term, the forces are computed in two steps. Firstly, forces excluding the viscous force are computed, and then the viscous force is computed implicitly. In our study, viscous forces are derived based on kinematic viscosity to ensure a symmetric matrix even in multi-phase flows. We utilize the Conjugate Gradient method to solve the sparse matrix, employing a Jacobi preconditioner due to its strongly diagonal dominant characteristics.

$$\boldsymbol{u}_i^{n+1}\left[1 - \sum_j K_{ij}^n \Delta t\right] + \sum_j K_{ij}^n \boldsymbol{u}_j^{n+1}\,\Delta t = \boldsymbol{u}_i^{n,p} \tag{10}$$

$$K_{ij}^n = \overline{v_{ij}^n} \frac{2r_{ij}^n \cdot \nabla_i W_{ij}}{\left(\left|r_{ij}^n\right|^2 + \eta^2\right)} \frac{m_j}{\rho_j^n} \quad (11)$$

3. Numerical Investigation

The VULCANO VE-U7 test stands out as a unique experiment designed to observe different spreading behaviors based on the substrate material [5]. Its distinctive design makes it one of the most renowned benchmark experiments in corium spreading research. In this section, we provide a brief summary of the VULCANO VE-U7 experiment and present the results obtained.

3.1 VULCANO VE-U7 Experiment

The VULCANO VE-U7 experiment is conducted within the VULCANO facility, operated by the PLINIUS experiment platform at CEA Cadarache, utilizing prototypic corium. In this experiment, corium enters the furnace and flattens in a stabilization pool to prevent the formation of droplets. Subsequently, it bifurcates into ceramic and concrete channels as in Fig.2. According to the experimental findings, on the inert ceramic substrate, corium stopped at a distance of 46cm, while in the concrete channel interacting with corium, corium stopped at 36cm from the bifurcation point [5].

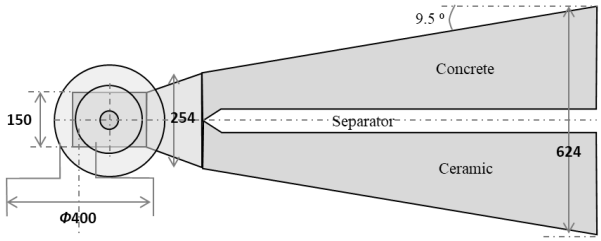

Fig. 2. Test section of VULCANO VE-U7 experiment

The initial melt temperature is set at 2450°C, while the initial substrate temperature is maintained at 300°C. A total of 40.8kg of melt is evenly distributed into both channels at a constant flow rate of 4.3kg/s. The geometric conditions and physical properties employed in this study are derived from previous research [2]. Notably, concrete ablation and natural convection effects are neglected in our analysis due to their minimal impact. Additionally, pseudo-solidification is modeled utilizing the Ramacciotti viscosity model [5].

3.2 Single-Channel Analysis

Firstly, the convergence of numerical methods is validated in single inert ceramic channel. The analysis was performed for 5 different spatial resolution. Initially the trend is similar to isothermal spreading. As time progresses, bulk region is cooled and it leads to the termination of spreading behavior, consistent with experimental observations. The results with a particle spacing of 2.5mm are illustrated in Figure 3, while the comparison with experimental results is depicted in Figure 4. Overall, the simulations exhibit excellent convergence, and cases with particle spacings of 5mm and below are nearly overlapping.

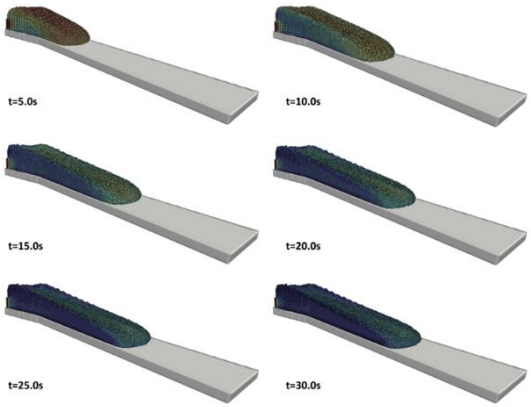

Fig. 3. Time evolution of corium in single inert ceramic channel

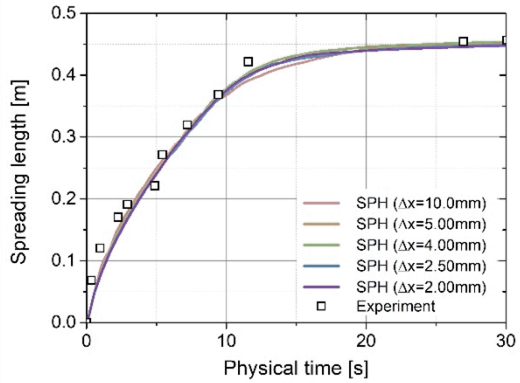

Fig. 4. Time evolution of spreading length in different spatial resolution compared to experiment.

3.2 Full-Channel Analysis

In this section, numerical simulations are conducted on a broader domain encompassing both the concrete channel and the stabilization pool. Unlike inert ceramic substrates, the response of molten corium interacting with concrete substrates (MCCI) must be considered. Previous studies have indicated that gas generation from the interaction between molten corium and concrete can increase corium viscosity and intensify convective heat transfer. Additionally, gas generation can lead to the solidification of corium with porosity, augmenting its effective area and enhancing radiative heat transfer. Recent studies have also suggested that corium may slip on the gas layer at the bottom [2].

In this study, we conducted tests to investigate the effects of changes in viscosity, convection heat transfer, and slip motion. However, resolving all these aspects on a small scale is impractical, and the exact properties of corium are not fully known. Therefore, we conducted sensitivity analyses by adjusting macroscopic parameters to demonstrate the effects of gas generation. To observe the enhanced convective heat transfer effect, the effective conductivity was increased. To observe increased viscosity, viscosity was simply increased. To investigate the effect of slip motion on the gas layer, a Navier slip boundary condition was applied.

The results are shown from figure 5 to 7 with brief explanation. As heat transfer enhances in the concrete channel, the temperature in the bulk decreases rapidly, and shorter spreading length is shown. Increasing viscosity result in a shorter spreading length from the beginning which is different from experiment. Allowing slip at the concrete result in a early progression of concrete compared to ceramic, consistent with experiment results. The post-MCCI response of corium properties remains uncertain, but the results might be formed due to combination of these various influences.

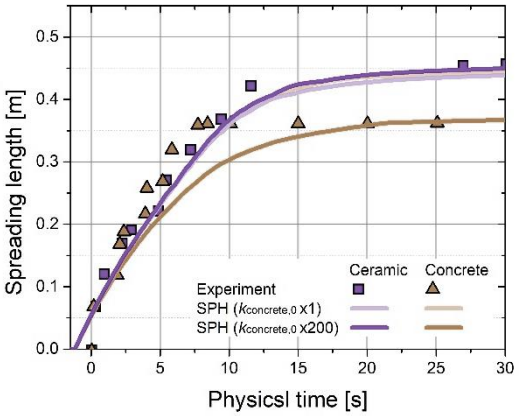

Fig 5.Time evolution of spreading length of both channel with enhanced heat transfer

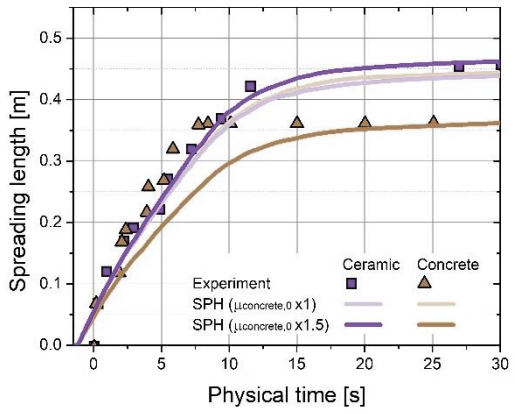

Fig 6.Time evolution of spreading length of both channel with increased viscosity

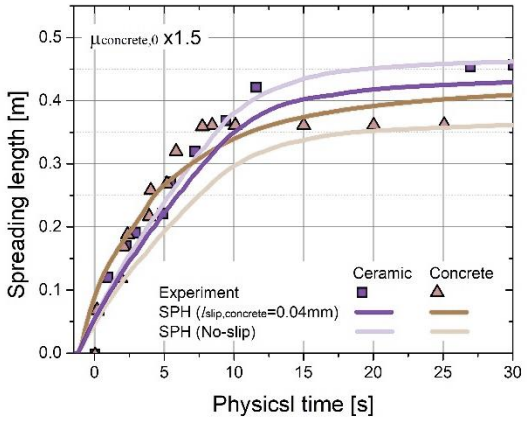

Fig 7.Time evolution of spreading length of both channel with slip motion

4. Conclusion

In this study, we numerically investigate the corium spreading phenomena using the SPH method. To ensure both efficiency and accuracy in our results, we augment the conventional SPH approach with the ALE method and an implicit viscosity solver.

In the analysis of single inert ceramic channel, we achieve convergence of the spreading length with experimental results and thoroughly examine the comprehensive spreading motion of corium. For the full-channel analysis, which includes the concrete channel reacting with corium, we conduct sensitivity studies to investigate the effects of changes in thermal-hydraulic physical properties by gas generation from MCCI response. In these studies, we meticulously examine the motion of corium in both channels, taking into account various factors and their interactions.

ACKNOWLEDGEMENGS

This work was supported by the National Research Foundation of Korea(NRF) grant funded by the Korea government(MSIT). (No. 2021M2D2A1A03046881)

REFERENCES

[1] Na, H., Kim, H. S., Lee, H. J., Kim, D. S., & Kwon, S. (2017). Preliminary feasibility study of post-flooding ex-vessel corium cooling strategy by CFD spreading simulations and concrete ablation analysis. Progress in Nuclear Energy, 97, 139-152.

[2] Duan, G., Yamaji, A., Journeau, C., Buffe, L., & Haquet, J. F. (2020). Investigation on corium spreading over ceramic and concrete substrates in VULCANO VE-U7 experiment with moving particle semi-implicit method. Annals of Nuclear Energy, 141, 107266.

[3] Morikawa, D., Senadheera, H., & Asai, M. (2021). Explicit incompressible smoothed particle hydrodynamics in a multi-GPU environment for large-scale simulations. Computational Particle Mechanics, 8, 493-510.

[4] OGER, Guillaume, et al. SPH accuracy improvement through the combination of a quasi-Lagrangian shifting

transport velocity and consistent ALE formalisms. Journal of Computational Physics, 2016, 313: 76-98.

[5] Journeau, C., Boccaccio, E., Brayer, C., Cognet, G., Haquet, J. F., Jégou, C., ... & Monerris, J. (2003). Ex-vessel corium spreading: results from the VULCANO spreading tests. Nuclear Engineering and Design, 223(1), 75-102.